Quality Parameters of Digital Terrain Models

Wilfried Karel[ς]
Christian Doppler Laboratory for
"Spatial Data from Laser Scanning and Remote Sensing" at the I.P.F.
Vienna University of Technology, Austria

Karl Kraus[σ]
Institute of Photogrammetry and Remote Sensing (I.P.F.)
Vienna University of Technology, Austria

1. Introduction

Quality parameters of Digital Terrain Models (DTM) are a hot topic today. This article presents both global and local quality parameters.
Using check points, global quality parameters are determined for a specific measurement technique, for instance airborne laser scanning (ALS), or digital stereo photogrammetry. They describe the whole area of interest with a few parameters only.
In contrary to global quality parameters, local ones describe the quality of a DTM at a high level of detail. The local parameters given in this paper describe the quality of each grid point of a DTM.
In section 6, an ALS project is confronted with a photogrammetric one in the same area through local quality parameters.

2. Global Quality Parameters

A formula that describes the height accuracy of topographic measurements is more than a hundred years old. It stems from Carl Koppe:

$$\sigma_H = \sigma_Z + \sigma_G \tan\alpha \tag{1}$$

σ_H … standard deviation in height of topographic maps, nowadays of DTM [Kraus, 2004]
σ_Z … standard deviation in height of measurement
σ_G … standard deviation in planimetry of measurement
α … terrain slope

It has to be mentioned that from the point of view of error propagation, variances should be used instead of standard deviations. However, standard deviations are used in rules of thumb, and (1) is not more than that.

2.1. Stereo Photogrammetry

If applied for stereo photogrammetry, (1) has to be used in the following form [Kraus, 2004]:

$$\sigma_H = \pm\left(0.15‰ \text{ of } h + \frac{0.15}{c}\, h \tan\alpha\right) \tag{2}$$

[ς] wk@ipf.tuwien.ac.at
[σ] kk@ipf.tuwien.ac.at

h … flying height

c … principal distance of the camera [mm]

Formula (2) may only be applied for open terrain. In case of wooded areas, uncertainty increases by approximately 2m.

Example: h = 1500m, c = 15cm, 10% terrain slope

$$\sigma_H = 0.22 + 1.5 \cdot 0.1 = \pm 0.37m \quad \text{open terrain} \\ \pm 2.4m \quad \text{wooded areas} \tag{3}$$

2.2. Airborne Laser Scanning

For ALS, the following formula must be used:

$$\sigma_H [cm] = \pm \left(\frac{6}{\sqrt{n}} + 50 \tan \alpha \right) \tag{4}$$

n … points per square meter

Unlike in photogrammetry, the flying height does not affect DTM height accuracy in today's airborne laser scanning. For ALS, point density is the critical influencing factor. However, future scanners will allow for a larger variability in flying height. Thus, planimetric point errors stemming from angular measurement errors of the inertial measurement unit will become distinguishable. This factor will be considered in the second term that describes the impact of planimetric errors on DTM height accuracy.

Example: 2m point spacing, 10% terrain slope

$$\sigma_H = \pm \left(\frac{6}{\sqrt{0.25}} + 50 \cdot 0.1 \right) = \pm 17cm \quad \text{open terrain, 100\% penetration rate} \\ = \pm \left(\frac{6}{\sqrt{0.0625}} + 50 \cdot 0.1 \right) = \pm 29cm \quad \text{wooded terrain, 25\% penetration rate} \tag{5}$$

The two constants 6 and 50 were determined using more than 22.000 check points in mountainous and slightly sloped terrain. The height differences between the check points and the DTM were analysed. These residuals were classified according to the terrain slope and the ALS data density at the respective check point, see Fig. 1.

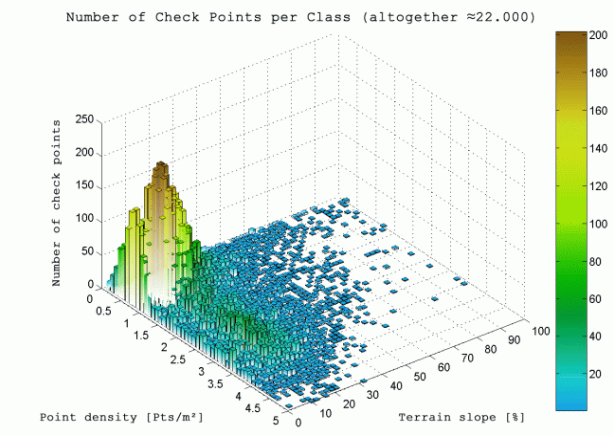

Fig. 1. In order to determine the two constants of formula (4), the residuals in height between 22.000 check points and corresponding ALS DTM were classified according to local terrain slope and data density. Using the standard deviation of each class, the constants of the quality formula were computed in an adjustment.

Subsequently, the standard deviation was computed for each class of residuals. Using these standard deviations as observations, the two constants of equation (4) were determined in an adjustment.
The derived constants already hold high stability. Nevertheless, they are enhanced every time new data is available to the author.
Other alternatives to equation (4) were investigated, like adding a constant term, using terms of higher degrees, or the summation of variances instead of standard deviations. None of the corresponding adjustments yielded convincing results.

3. Transitional Remarks

Spectral analysis with test profiles resides in an intermediate position between global and local quality parameters, confer [Tempfli, 1980], or [Frederiksen, 1980]. However, according to [Li, 1993], spectral analysis has not found its way to practice.
Another method, which was a focus of the EuroSDR seminar in Aalborg, is interesting mainly from the point of view of automatic DTM enhancement. Overlapping digital orthophotos are generated using the (flawed) DTM. The resulting parallaxes in the orthophotos are a measure for the height accuracy of the DTM. In place of the generation of orthophotos, also a back projection can be done [Schenk, 2005].
Alternatively, quality measures may be derived by error propagation. However, users experience this technique as a black box, as no information is given on the impacts of individual factors on quality. Furthermore, this method is not applicable to existing DTM, which is a very important task these days.
As an alternative to error propagation, an empirical, stochastic **step-by-step** approach has been developed that generates very detailed quality measures.
This step-by-step approach can be characterized as follows: it is

- **applicable** in a post-processing phase **to any DTM** existing beforehand, it is
- **independent of** the DTM **interpolation method**, it
- uses the **original data** (ALS: without eliminated points on trees and buildings), it produces quality measures
- in the **resolution** of the individual **grid points**, and it
- provides **attractive visualizations**.

4. Local Quality Measures

The first parameter of the aforementioned step-by-step approach is the density of the original points $\overline{n}$. It is computed as the density in the cells of a regular grid covering the area of interest.
The next local quality measure is the distance c_{m_i} between each grid point and the data point next to it (Fig. 2). This parameter may be computed efficiently using the Chamfer function [Borgefors, 1986].

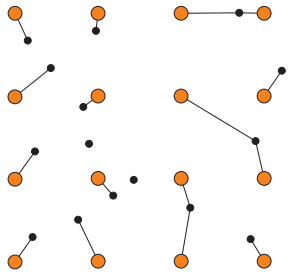

Fig. 2. The distances between each grid point (orange) and the data point next to it (black) are of great importance for DTM quality.

DTM curvature also holds large effects on the quality measure. First, curvatures at each grid point are computed along the grid lines, considering break lines (Fig. 3). Now, maximum and minimum main curvatures are deduced, and with these, the curvature $1/r_{\alpha_i}$ in an arbitrary direction α_i can be given.

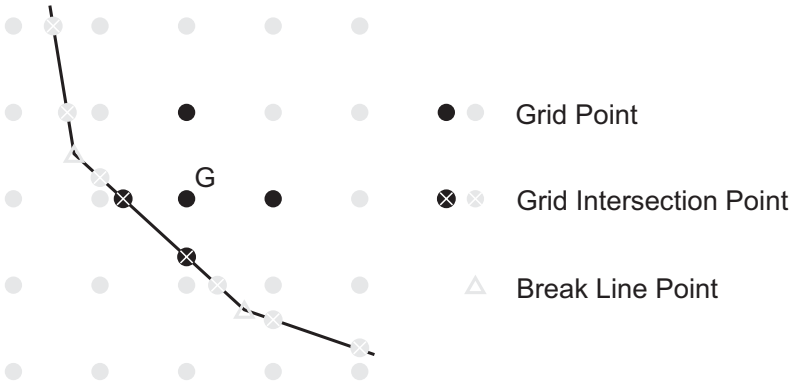

Fig. 3. Computation of the curvature at grid point G : points used are coloured black.

With both the original data used for DTM generation and the DTM itself, accuracies can be computed that are representative for the surrounding data points of a grid point G. A weighted $RMSE$ (6) is used that is calculated using the discrepancies in height d_i between the original data and the DTM surface (Fig. 4). If the $RMSE$ results smaller than the a priori known standard deviation of measurement, it is replaced by that value.

$$RMSE = \sqrt{\frac{\sum_i d_i d_i p_i}{\sum_i p_i}} \tag{6}$$

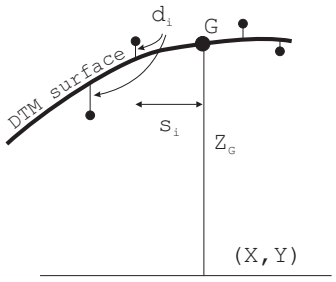

Fig. 4. Discrepancies in height d_i between the DTM surface and the original data points.

The weights p_i are defined as follows:

$$p_i = \frac{1}{1 + s_i^2 / r_{\alpha_i}^2} \tag{7}$$

s_i … distance grid point – original point
r_{α_i} … radius of curvature of the DTM at the original point towards the grid point

These weights have the effect that the nearer the data point is to the grid point G, the more influence on the $RMSE$ it gets. An analogical effect has curvature. By assigning an adequate threshold, the neighbourhood of a grid point G may be delimited. Using the information

stated above, DTM height accuracies can be computed. Left to answer is the question which interpolation method to take. As for accuracy estimates rather simple interpolation methods can be chosen, the authors decided to apply moving least squares (MLS) with an order one polynomial (plane), weighted with (7). In order to ease computation, each plane is calculated in an own coordinate system whose z-axis goes through the grid point (see Fig. 5).

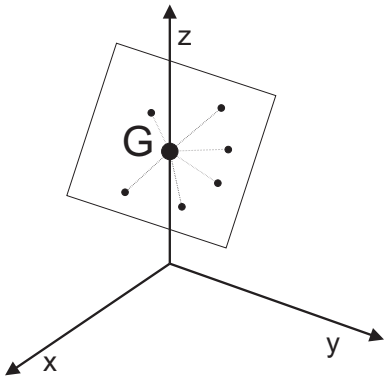

Fig. 5. Adjustment of a plane using the surrounding data points of grid point G, having defined the z-axis going through G.

The standard deviation $\hat{\sigma}_{z_G}$, which we name $\hat{\sigma}_{DTM}$, is computed as [Kraus et al., 2005]:

$$\hat{\sigma}_{DTM} = RMSE \cdot \sqrt{q} \tag{8}$$

Where q is the cofactor in height of the least squares adjustment of the tilted plane. If q is 1, then the DTM grid point holds the same accuracy as the surrounding data points. If the cofactor is larger than 1, then the grid point owns an accuracy that is worse than the ones of the neighbouring data points. Reasons for that may be large distances or high curvatures to the next data points. If q is smaller than one, which should be aimed at, then the DTM holds higher accuracy than the surrounding data points. In the paper [Kraus et al., 2005], there are given further details on this theory. Moreover, it presents a drastic example with large data voids, as they may occur in the practice of ALS.
In the next section the quality measures of a high alpine ALS DTM are presented. In the subsequent section a DTM generated with photogrammetric data is confronted with an ALS DTM of the same area of interest.

5. Local Quality Parameters of an ALS Project

The mountainous area of the ALS project described in this section resides in Montafon, Vorarlberg, Western Austria. It covers 1500 by 1100 meters. Height ranges between 1700 and 2600m above sea level. See a shaded view of the digital surface model in Fig. 6.

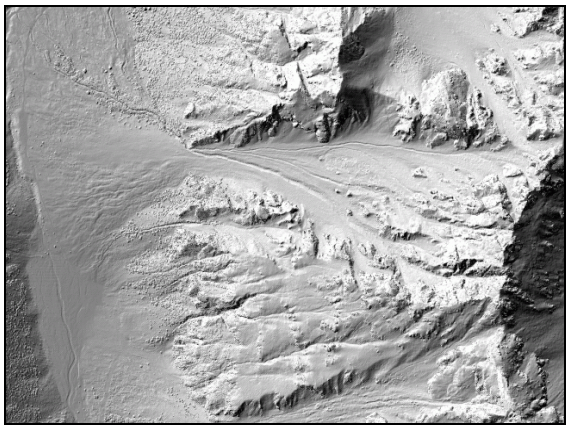

Fig. 6. Shaded digital surface model, derived from all ALS points. Rocky terrain with relatively few vegetation is visible. Project of the "Landesvermessung Vorarlberg".

Data capture is done with a mean point density of ≈2 points per square meter. Using robust filtering, 3.6 million points are classified as terrain points, see Fig. 7.

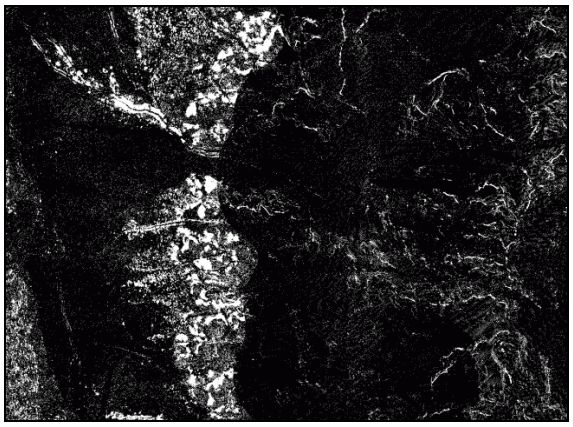

Fig. 7. Classified terrain points (black) of the Montafon project.

Using the classified terrain points, the DTM is interpolated with a grid width of 1m through the linear prediction calculus implemented in the software SCOP++. See a shaded view of the DTM together with derived contour lines on Fig. 8.

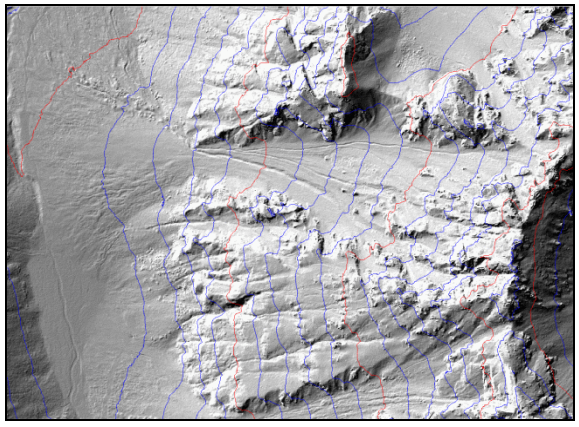

Fig. 8. Shaded DTM together with derived contour lines every 25 meters. The DTM bases on the ALS points classified as terrain points through robust filtering (Fig. 7).

As a first quality check, point density is computed. Data characteristics become obvious in the respective colour-coded image (Fig. 9). The broad band of high density in North-South direction stems from the overlap of two laser scanner strips. The three narrow bands of high density in East-West direction are oriented perpendicularly to the flight path and do not correspond to terrain characteristics. They may stem from turbulences during the flight.

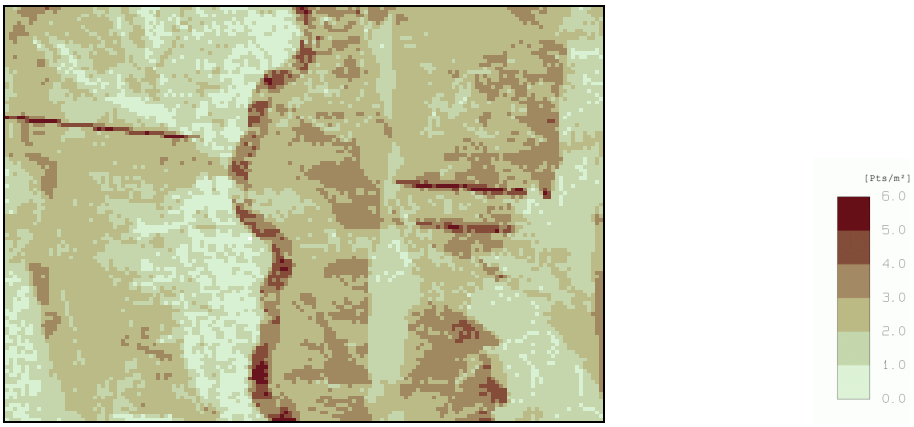

Fig. 9. Density of classified ALS terrain points, computed with a cell size of 100m².

By applying the chamfer function, the distance from each grid point to its nearest data point is computed. Now, the data voids get visible, which users should be warned of. Thus, grid points that are further away from point data than seven times the DTM grid width, are coloured red (Fig. 10).

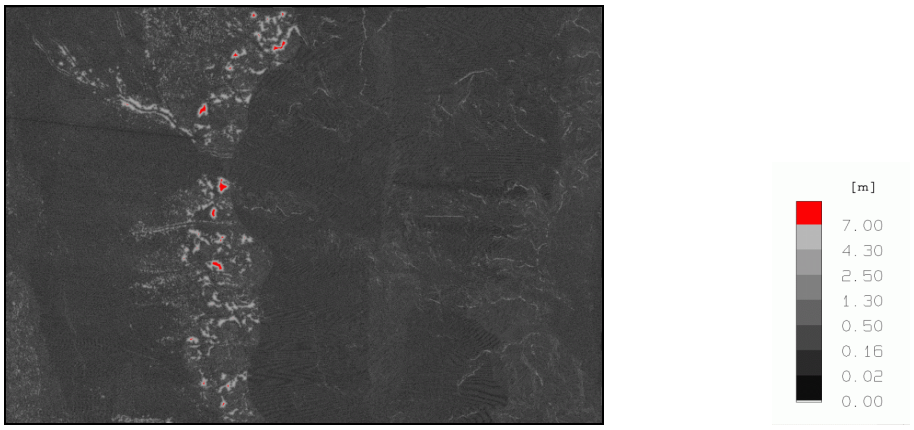

Fig. 10. Distance from each grid point to its nearest data point (see Fig. 2). Grid points with larger distances than seven times the DTM grid width (≙7m) are coloured red.

The maximum main curvatures at the grid points (Fig. 11) show up fine terrain characteristics. Crests and rifts become visible. Obviously, this measure is a good representation of the terrain's geomorphology.

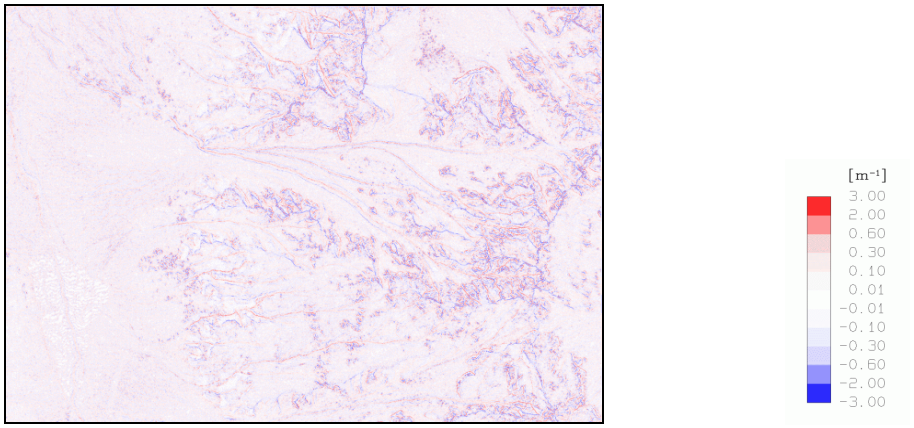

Fig. 11. Maximum main curvatures at the grid points (see Fig. 3).

The colour-coded image of the weighted root mean square error *RMSE* in Fig. 12 presents the local accuracy of the data points. Lowest values occur in the non-vegetated, plane zones,

while the *RMSE* reaches values of up to 5m along the crests. Grid points determined as unusable (Fig. 10) are marked red.

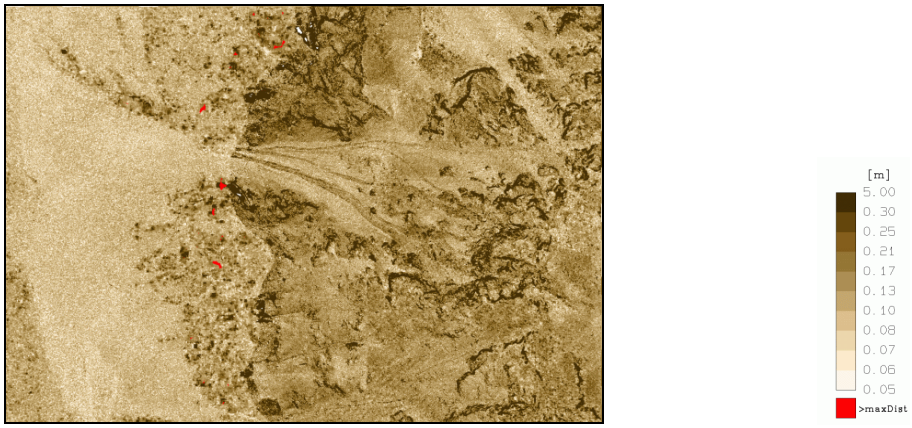

Fig. 12. *RMSE* at each grid point (see (6), (7), and Fig. 4).

The cofactor in height (Fig. 13) mainly varies around 0.3. Along the crests and in the data voids, values of up to 1 show up. Moreover, the overlap of the two laser scanner strips is distinguishable (compare Fig. 9). Once again, unusable areas are coloured red (see Fig. 10).

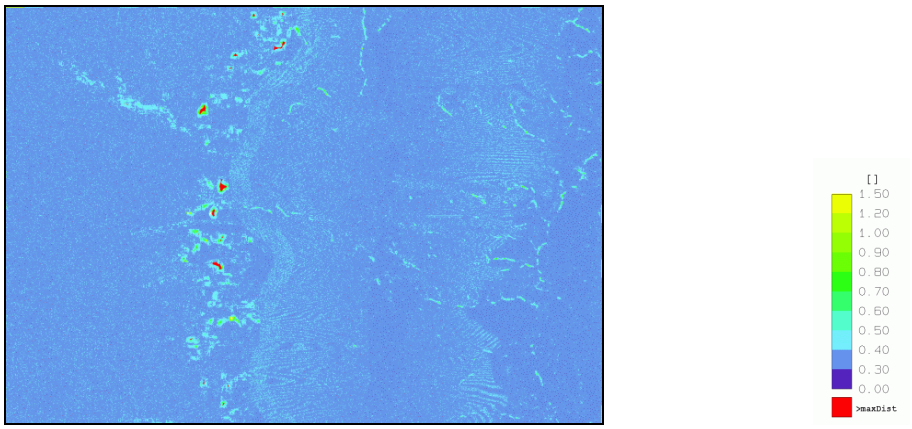

Fig. 13. Cofactor at each grid point (see (7), and Fig. 5).

Finally, $\hat{\sigma}_{DTM}$ is computed (Fig. 14). DTM height accuracies around 4cm result in the non-vegetated, plane areas. In the vegetated zones, variation increases with values up to 30cm. Worst accuracies are achieved along the crests. Unusable areas (see Fig. 10) are once again marked red.

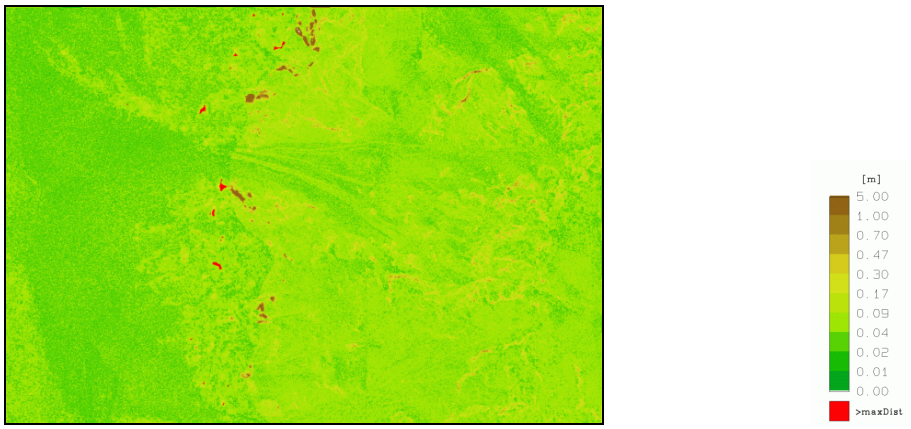

Fig. 14. DTM height accuracy at each grid point (see (8)).

6. Comparison of ALS and Photogrammetry

The slightly sloped area treated in this section is located in the Haselgraben, Upper Austria. It is described by both a photogrammetric and an ALS DTM, whereupon the ALS data was captured with about 1m mean point spacing. The photogrammetric data stems from an aged, countrywide data set that was captured at a scale of 1:30.000 (bulk points), or 1:15.000 (structure information), respectively [Franzen & Mandlburger, 2003].
Fig. 15 gives an impression of the test site, as it presents a shaded view of the ALS surface model.

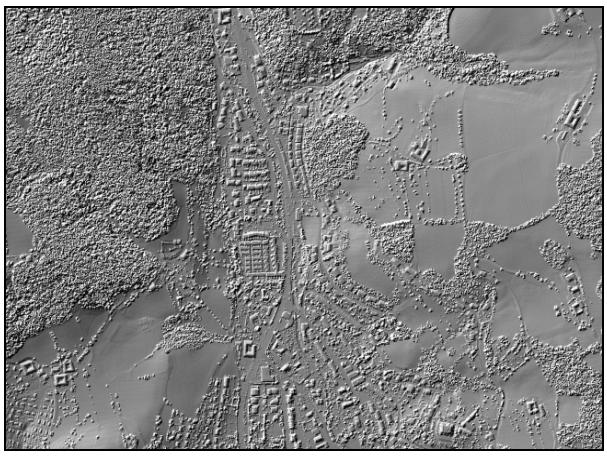

Fig. 15. Shaded digital surface model of the ALS DTM of the Haselgraben test site. Project of the "Oberösterreichische Landesvermessung".

The data sets used as input for DTM interpolation are presented in Fig. 16. The ALS points were classified by robust filtering. Large data voids mainly stemming from buildings show up. The photogrammetric data consist of homogeneously distributed bulk points and additional break and form lines with a high level of detail.

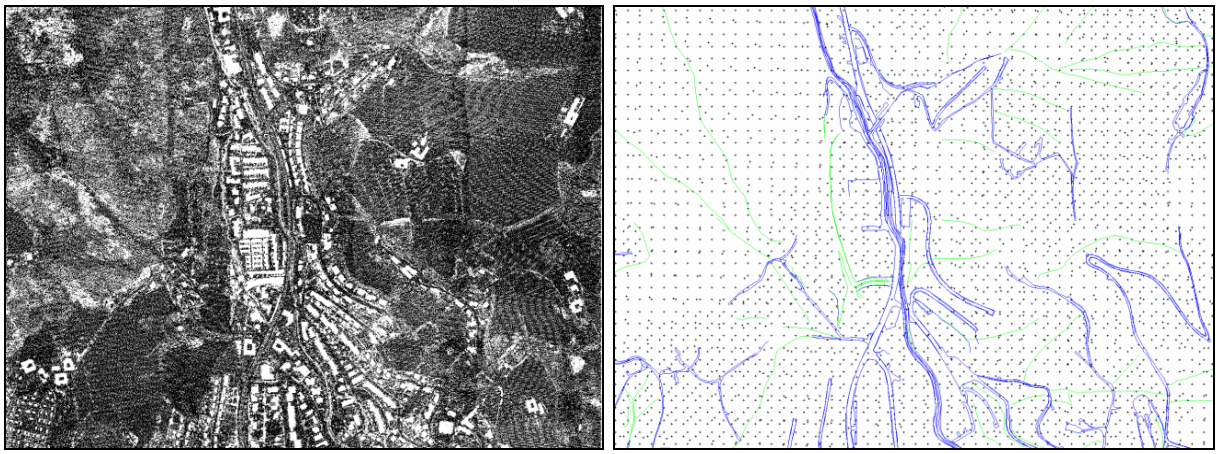

Fig. 16. Input data for the interpolation of the ALS (left) and the photogrammetric (right) DTM. Break lines in the photogrammetric data set are coloured blue, form lines are green.

In Fig. 17, the resulting DTM are presented in shaded views. The ALS DTM has a grid width of 1m and shows up high detail throughout the whole area. The photogrammetric DTM holds a grid width of 10m and is based on bulk points with much larger point spacing. However, through the selective, manual measurement of structure information, the topographically interesting elements are also described by the photogrammetric DTM, at a comparable level of detail. Obviously, the photogrammetric DTM contains some blunders along the inclination in the Northwest. It has to be mentioned that these errors could widely be corrected during a review, leading to an enhanced countrywide DTM [Franzen & Mandlburger, 2003].

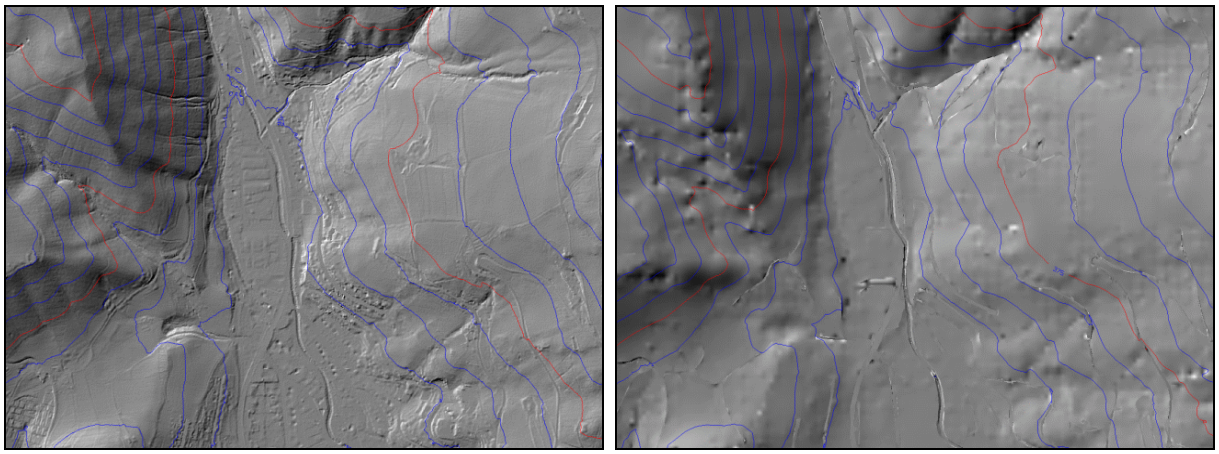

Fig. 17. Shaded ALS (left) and photogrammetric (right) DTM together with contour lines every 25 meters.

The data densities of the two DTM (see Fig. 18) show up that the ALS DTM is covered by four overlapping laser scanner strips, leading to an area of high density in the form of a T standing upside down. The data density of the photogrammetric DTM varies mainly due to additional structure information.

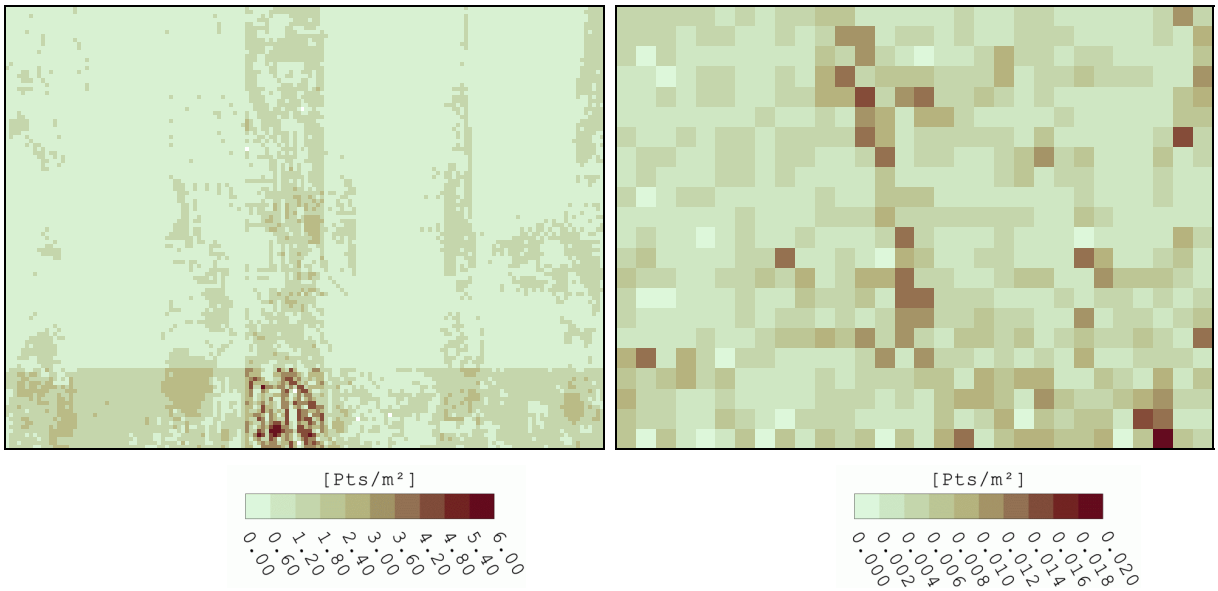

Fig. 18. Point densities, calculated with a cell size of 100m² (ALS, left), and 250m² (photogrammetry, right). Please note that two different colour tables are used.

Data voids of the ALS data, generated by robust filtering show up in the colour-coded view of the distance from each grid point to its nearest data point (Fig. 19, left). Distances larger than seven times the grid width are marked red, in order to warn users. The corresponding image of the photogrammetric data (Fig. 19, right) owns an outstanding pattern of extreme distances. It stems from the difference between the bulk point spacing of about 25m and the DTM grid with of 10m, which was chosen according to the higher level of detail of structure information.

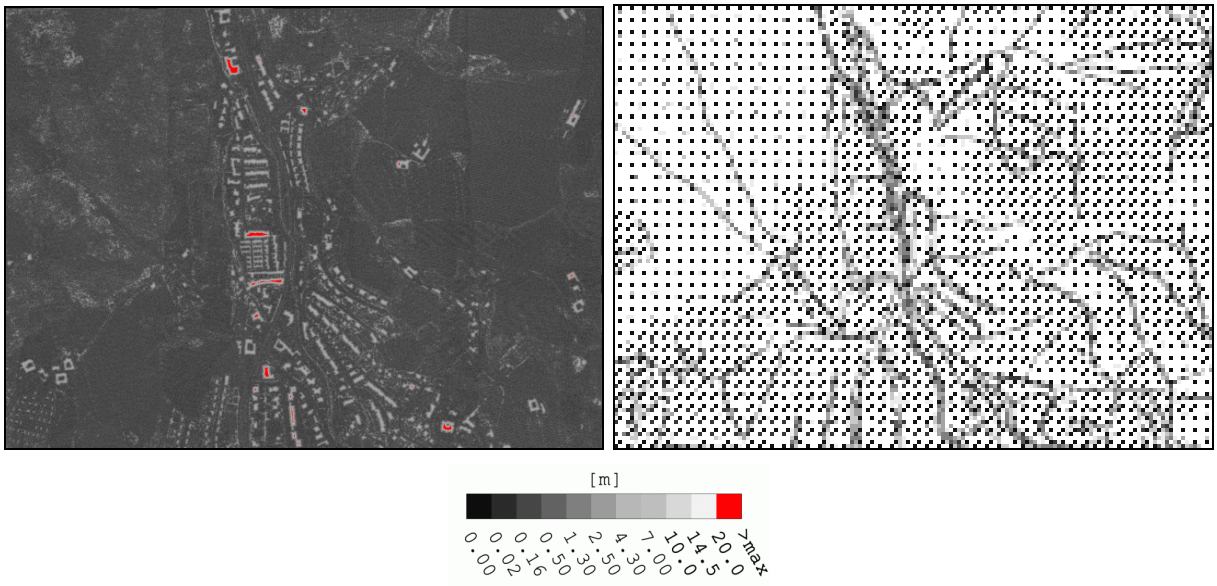

Fig. 19. Distance to nearest data point. In the ALS DTM (left), distances larger than 7m are coloured red. For the photogrammetric DTM (right), an outstanding pattern is noticeable that stems from the difference between the bulk point spacing and the DTM grid width.

Fig. 20 presents the maximum main curvatures at the grid points. The images of the curvatures of both DTM show comparable results. As break lines are considered in the computation of curvature, extreme values mainly occur around form lines of the photogrammetric data set.

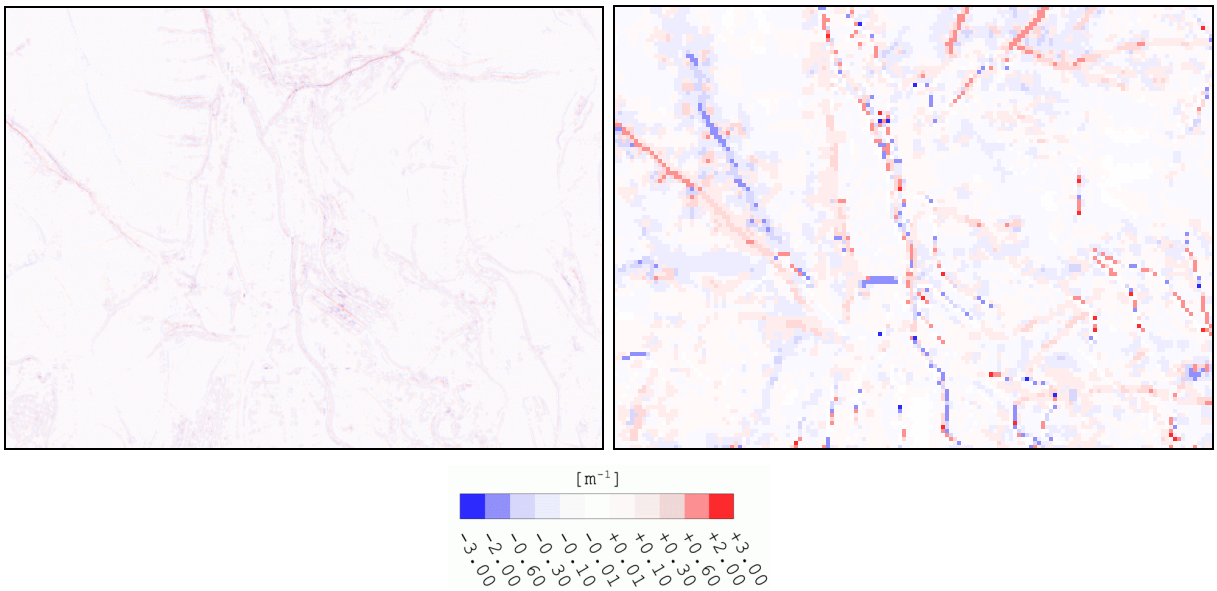

Fig. 20. Maximum main curvature at each grid point of the ALS (left) and the photogrammetric (right) DTM.

The local, weighted *RMSE* of the input data are presented in Fig. 21. For the ALS DTM, values result as near to the standard deviation of measurement (given as ±5cm), except for terrain breaks, and vegetated zones. For the photogrammetric DTM, the *RMSE* show up the data blunders.

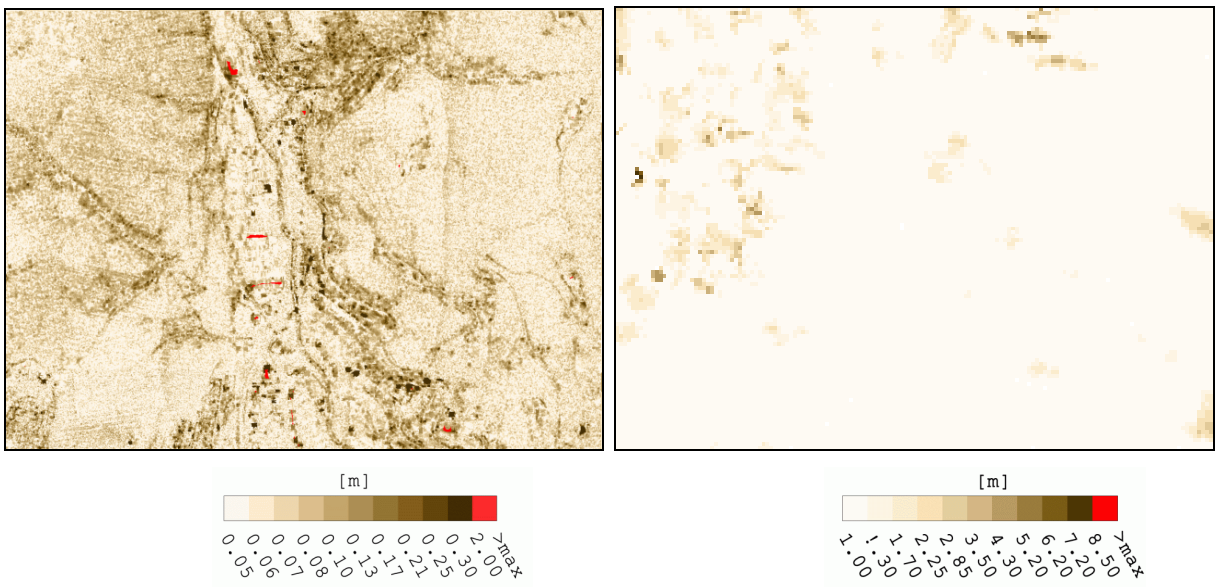

Fig. 21. Weighted *RMSE* of the ALS (left) and the photogrammetric (right) DTM. The *RMSE* in the photogrammetric DTM are widely replaced by the a priori known standard deviation of measurement (±1m). Grid points determined as unusable (see Fig. 19) are marked red. Please note that two different colour tables are used.

The cofactors in height (see Fig. 22) show up different characteristics of the data. For the ALS DTM, mainly the overlaps of the laser scanner strips are distinguishable. For the photogrammetric DTM, the cofactors own a much higher variation stemming mainly from inconsistencies between the bulk data and the additional structure information.

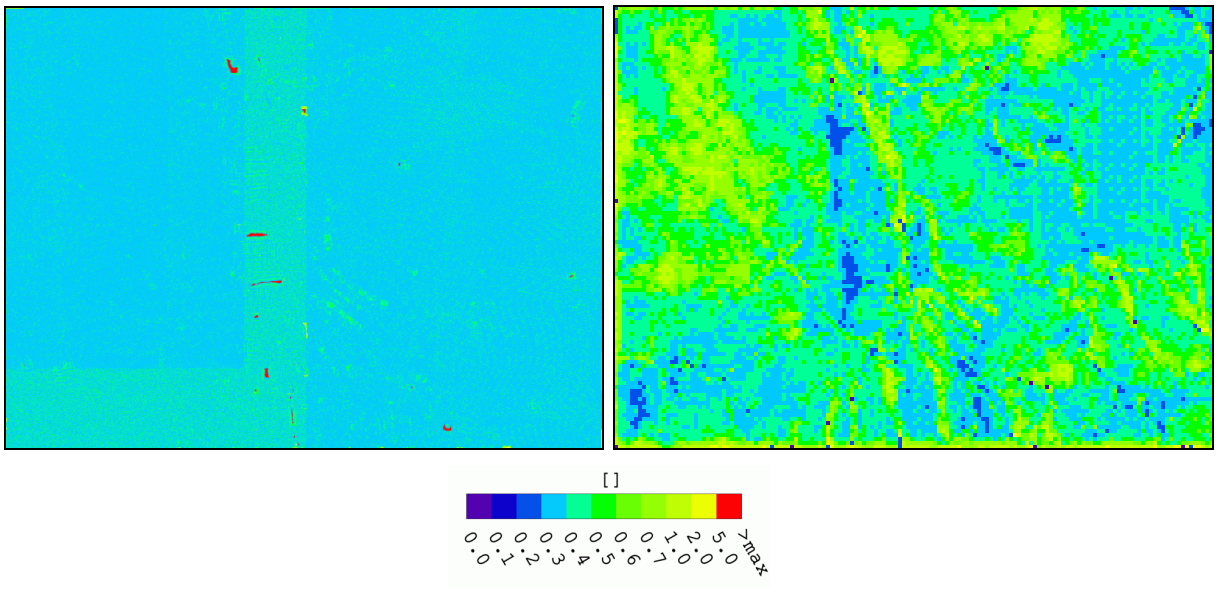

Fig. 22. Cofactors in height of both DTM (ALS: left, photogrammetry: right). Unusable areas (see Fig. 19) are marked red.

The resulting DTM height accuracies are presented in Fig. 23. The quality of the ALS DTM is much better than the one stemming from photogrammetric data. While the accuracy of the ALS DTM is better than 4cm over wide areas, the photogrammetric DTM mainly holds an accuracy of worse than 0.5m, and even reaches values of worse than 5m.

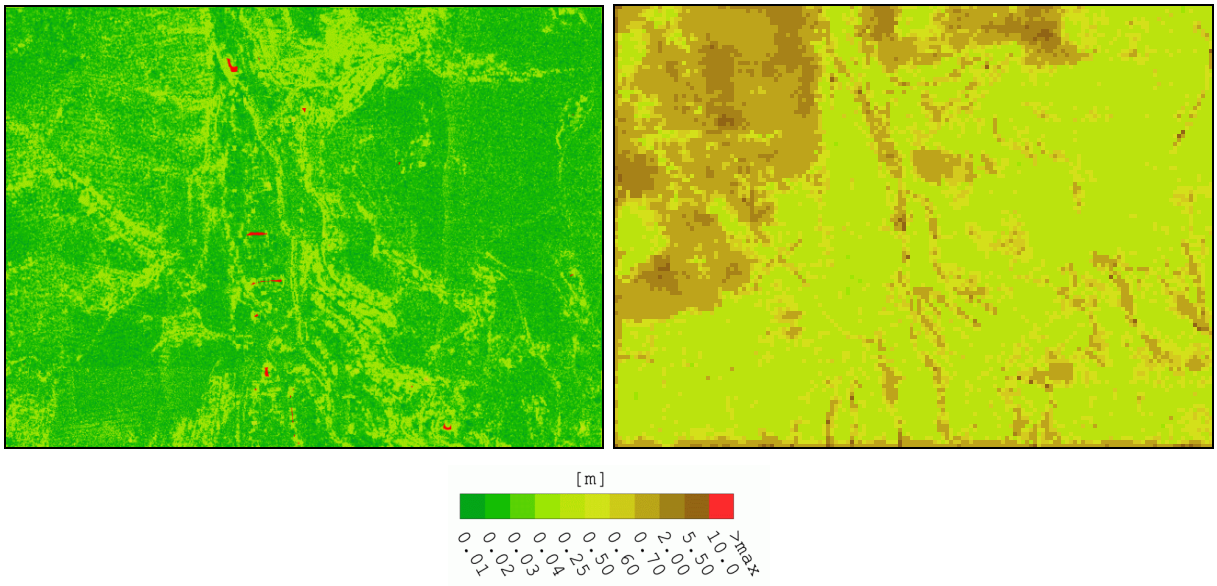

Fig. 23. DTM height accuracy at each grid point (ALS: left, photogrammetry: right). Unusable areas (see Fig. 19) are marked red.

7. Conclusions and Outlook

Global quality parameters for DTM derived from ALS or photogrammetric data are known by empirical analyses. These global parameters are important for the management of DTM projects.

An approach to derive local DTM quality measures has been developed that holds major advantages in comparison to other methods and generates promising results. Local DTM quality may be expressed by:

- point density
- distance between each grid point and its nearest data point
- curvature
- weighted root mean square error of the surrounding original data (*RMSE*)
- standard deviation of each grid point $\hat{\sigma}_{DTM}$

The next step is the improvement of software performance. Afterwards, the approach has to be tested with more data sets, which will generate a feedback for improving the theory and the implementation.

In the future, DTM should be handed over to users together with the presented local quality parameters, at best in terms of quality layers.

8. Bibliography

Borgefors, G., 1986. Distance Transformations in Digital Images. Computer Vision, Graphics and Image Processing, CVGIP 34 (3), pp. 344-371.

Franzen, M. & Mandlburger, G., 2003. Die neue Generation des digitalen Geländemodells von Österreich. VGI 03/2003.

Frederiksen, P., 1980. Terrain Analysis and Accuracy Prediction by Means of the Fourier Transformation. International Archives of Photogrammetry and Remote Sensing, 23(4); 284-293.

Kraus, K., 2004. Photogrammetrie. Band 1: Geometrische Informationen aus Photographien und Laserscanneraufnahmen, 7. Auflage, Walter de Gruyter, Berlin., Germany, 397 pages.

Kraus, K., Karel, W., Briese, C., Mandlburger, G., 2005. Quality Measures for Digital Terrain Models. Photogrammetric Record, under review.

Li, Z., 1993. Theoretical Models of the Accuracy of Digital Terrain Models: an Evaluation and Some Observations. Photogrammetric Record, 14(82): 651-660.

Schenk, T., 2005. The back projection method. Presentation at the EuroSDR seminar in Aalborg on automated checking of DTM, August 2005.

Tempfli, K., 1980. Spectral Analysis of Terrain Relief for the Accuracy Estimation of Digital Terrain Models. ITC Journal 1980-3: 478-510.